Pharm Res (2014) 31:1185–1193
DOI 10.1007/s11095-013-1241-y

RESEARCH PAPER

# Investigation of the Influence of Nephropathy on Monoclonal Antibody Disposition: A Pharmacokinetic Study in a Mouse Model of Diabetic Nephropathy

Frank A. Engler • Bo Zheng • Joseph P. Balthasar

Received: 5 August 2013 / Accepted: 20 October 2013 / Published online: 8 November 2013


## ABSTRACT

***Purpose*** This study employed a mouse model to evaluate the effects of diabetic nephropathy on the pharmacokinetics of 8C2, a murine monoclonal antibody (mAb).

***Methods*** Streptozotocin (STZ) was administered to mice to induce diabetic nephropathy (125 mg/kg/day × 2). Mice were grouped ($n$ = 8–10) based on time after STZ-treatment (control, 1, 2, 3, 4, or 6 weeks), and injected intravenously with 10 mg/kg 8C2. Blood samples were collected up to 7 days, and 8C2 plasma concentrations were determined via immunoassay. Inulin clearance and urinary albumin excretion rate (UAE) were determined to assess renal function.

***Results*** UAE, inulin clearance, and 8C2 clearance increased significantly following STZ. Comparing control and 6 week STZ-treatment groups, UAE and inulin clearance increased from 25.7 ± 3.3 to 99.3 ± 13.7 μg/day, and from 421 ± 31 to 584 ± 78 μl/min. 8C2 clearance increased from 121 ± 12.5 to 228 ± 61 μl/hr/kg ($p < 0.01$). 8C2 clearance was highly correlated with UAE ($r^2$: 0.731). Inclusion of UAE as a covariate in population modeling explained significant residual variability in 8C2 clearance.

***Conclusions*** The clearance of 8C2 increased significantly in STZ-treated mice. Population pharmacokinetic modeling suggests that UAE has potential for use in predicting mAb clearance in subjects with diabetic nephropathy, possibly assisting in the individualization of mAb dosing.

**KEY WORDS** diabetic nephropathy · antibody · pharmacokinetics · renal clearance · renal disease · streptozotocin

## ABBREVIATIONS

| | |
|---|---|
| CL | systemic clearance |
| GFR | glomerular filtration rate |
| IgG | immunoglobulin G |
| mAb | monoclonal antibody |
| STZ | streptozotocin |
| UAE | urinary albumin excretion rate |

F. A. Engler · B. Zheng · J. P. Balthasar (✉)
Department of Pharmaceutical Sciences
School of Pharmacy and Pharmaceutical Sciences
University at Buffalo, The State University of New York
452 Kapoor Hall, Buffalo, New York 14260, USA
e-mail: jb@buffalo.edu

## INTRODUCTION

There is substantial interest in the development of therapeutic monoclonal antibodies against a variety of targets in a multitude of diseases (1). Presently, 30 therapeutic monoclonal antibodies (mAb) are FDA approved (2), and hundreds are in development. These antibodies may find clinical application in almost every field of medicine.

As with all drugs, the kinetics of drug elimination play an important role in determining the relationships between the dosage rate of therapeutic antibodies and the extent of drug effect or toxicity. Many of the primary determinants of mAb elimination have been investigated in great detail. These determinants include the rate and extent of antibody entry into cells by fluid-phase pinocytosis (3–6), the binding and protection of immunoglobulin G (IgG) antibodies by the Brambell receptor (FcRn) (7–10), target-mediated clearance (11,12), and elimination of mAb through formation of immune complexes with host-generated anti-drug antibodies (13). Unfortunately, relatively little is known regarding the sources of interindividual variability in mAb clearance, and this variability may be substantial (e.g., >30% coefficient of variation on mAb clearance) (14).

Despite the very high perfusion rate of the kidney (~1.2 L/min in man) (15), and despite the importance of the kidney as an "elimination organ" for small molecule drugs, the kidney is commonly thought to play only a minor role in the elimination of mAb. In healthy individuals, the limited porosity and charge selectivity of the glomerular membrane leads to a very low efficiency of glomerular filtration of large proteins (16).

However, there is increasing evidence that some forms of renal disease, including diabetic nephropathy, lead to a substantial insult to glomerular selectivity and dramatically increase the renal elimination of IgG (17). For example, a 71 patient clinical study comparing healthy patients to Type 1 and Type 2 diabetic sample populations revealed that patients with type 2 diabetic nephropathy had nearly 200-fold higher concentrations of IgG2 in urine compared to healthy controls (18). In Pima Indians with type 2 diabetes and microalbuminuria (20–300 mg/dl) or macroalbuminuria (>300 mg/dl), there was a 4- and 80-fold respective increase in urinary IgG concentrations compared to individuals with normative urinary albumin excretion levels (19). In another study, patients with non-diabetic or diabetic nephropathy displayed a 75- or 130-fold increase in urinary IgG concentrations relative to control patients (20).

Although the above studies demonstrate that nephropathy leads to increased IgG excretion in the urine, there has been no direct investigation of impact of this elimination pathway on the systemic pharmacokinetics of mAb (to the authors' knowledge). However, the rigorous population modeling of ustekinumab pharmacokinetics in 1937 patients revealed that patients with diabetes had a 20% decrease in exposure compared to non-diabetic patients (21). Although markers of renal function were not measured in this study, it is possible that this finding relates to a substantial increase in the systemic clearance of ustekinumab in diabetic patients with nephropathy, through increased renal filtration and excretion.

To better understand the role of diabetic nephropathy on the systemic pharmacokinetics of mAbs, we have investigated the disposition of 8C2, a model murine IgG1 monoclonal antibody, with use of the streptozotocin mouse model of diabetes. Renal function was evaluated through assessment of inulin clearance and the rate of urinary albumin excretion (UAE). The intent of this work was to test the hypotheses that mAb plasma clearance is substantially increased in diabetic nephropathy, and that mAb plasma clearance correlates with UAE (which may be measured clinically to facilitate the *a priori* prediction of mAb clearance in diabetic subjects).

## MATERIALS AND METHODS

### 8C2 Production and Purification

8C2, a murine anti-topetecan IgG1 antibody, was utilized for this study. The mAb was generated from hybridoma cells and purified via Protein G affinity chromatography, as previously described (22). Briefly, 8C2 was purified from cell culture media with a BioLogic medium pressure chromatography system (Bio-Rad, Hercules, CA), attached to a 5 ml HiTrap Protein G HP column (GE Healthcare, Uppsala, Sweden). After loading of cell culture medium onto the column, the column was washed with 20 mM $Na_2HPO_4$ (pH 7.0), followed by elution with 100 mM Glycine buffer (pH 2.8). Samples were collected in 3 ml fractions into glass test tubes containing 100 µl of 1 M Tris buffer. Purified 8C2 was buffer exchanged into phosphate buffered saline with a 10 K MWCO Slide-A-Lyzer Dialysis Cassette (Pierce Biotechnology, Rockford, IL).

### Animals

Male Swiss Webster mice were obtained from Harlan Laboratories. Mice were housed in a temperature and humidity controlled environment with a standard light/dark cycle (12 h light/12 h dark), and mice were allowed free access to food and water. All animal protocols were in compliance with the Institutional Animal Care and Use Committee of the State University of New York at Buffalo Animal Facility regulations.

### 8C2 ELISA

8C2 Concentration was determined with an antigen specific Enzyme-Linked Immunosorbent Assay (ELISA). Briefly, a cationized bovine serum albumin-topetecan conjugate (cBSA-top) was synthesized through the use of a carbodiimide catalyzed amide bond reaction. cBSA-top dissolved in pH 9, 0.02 M $Na_2HPO_4$ at a concentration of 10 µg/ml was used to coat wells of Nunc Maxisorp 96 well plates (Nunc model # 62409–002, VWR, Bridgeport, NJ) at 4°C overnight (250 µl/well). The plates were washed with PB-Tween (0.05% Tween in 0.02 M $Na_2HPO_4$), followed by two washes of double distilled water. Plates were then incubated with standards and samples in triplicate (200 µl) for 2 h at room temperature. At the end of incubation, the plates were washed and then incubated with 100 µl of goat anti-mouse-Fab alkaline phosphatase conjugate (Sigma, Cat #A1682, St. Louis, MO) for 1 h at room temperature (1:500 dilution of the conjugate with PB-Tween with 30% BSA). After washing, p-nitro phenyl phosphate solution (Pierce, Rockford, IL), 4 mg/ml in diethanolamine buffer, pH 9.8, was added to each well (250 µl/well). The change in absorbance at 405 nm with respect to time (dA/dt) was measured (Spectra Max 340, Molecular Devices, Sunnyvale, CA), and standard curves were obtained by fitting dA/dt *vs*. 8C2 concentration using the linear equation: $y = mx + b$ (23).

### Determination of Glomerular Filtration Rate in Conscious Mice Using FITC-Inulin

FITC-inulin (Sigma Chemicals, St Louis, MO) was used to evaluate glomerular filtration rate (GFR) in conscious mice. This assay has been described previously (24). Briefly, 5% FITC-inulin was dissolved in 2 ml of 0.9% NaCl (Sigma Chemicals). To remove residual unbound FITC, the solution

was dialyzed with a 1KD cut-off dialysis membrane (Spectra/Pro 6, Spectrum Laboratories Inc., Rancho Dominguez, CA) for 24 h at room temperature. Prior to use, this dialyzed solution was sterile filtered through a 0.22 μm filter (Costar, Corning Inc., Tewksbury, MA). Three days prior to injection with 8C2, 5% FITC-inulin (3.74 μl/g body weight) was dosed retroorbitally under isoflurane-induced light anesthesia. After fully regaining consciousness, the mice were restrained inside a 50-mL centrifuge tube with large air-holes drilled in the tip. The inner thigh was closely shaven and wiped with 75% ethanol, revealing the saphenous vein. Approximately 20 μl blood is collected in a heparinized capillary tube (Fisher Scientific, Pittsburgh, PA) by venipuncture using a sterile 23 gauge syringe needle. Blood was sampled via the saphenous vein at 3, 7, 10, 15, 35, 55, 75 min post injection of FITC-inulin. Each plasma sample was buffered to pH 7.4, by mixing 10 μl of plasma with 40 μl of 500 mM HEPES (Fisher Scientific, Fair Lawn, NJ) (pH 7.4). The titrated samples were then loaded onto a 96-well plate, 50 μl sample/well. Fluorescence was determined using a Fluoroscan Ascent FL (Labsystems, FIN-00811 Helsinki, Finland), with 485 nm excitation, and read at 538 nm emission. Non-compartmental data analysis (WinNonlin 5.2, Pharsight, St. Louis, MO) was employed for the calculation of inulin clearance.

### Determination of Urinary Albumin Excretion in Mice

One day prior to dosing with 8C2, urine was collected from mice individually housed within metabolic cages, for assessment of albuminuria. Mouse urinary albumin excretion rate was determined by measuring the albumin concentration and volume of urine collected over 24 h. Urinary albumin concentration was determined using a commercially available indirect competitive ELISA kit (Exocell Inc., Philadelphia, PA).

### Study Design

Diabetes induced nephropathy was initiated by intraperitoneal injection of 125 mg/kg/day of STZ (Sigma, St Louis, MO) on two consecutive days. Control mice received injections of sterile saline. Mice were stratified into 6 groups (8–10 mice/group): Control, 1, 2, 3, 4, and 6 weeks post-dosing with STZ. FITC-Inulin clearance determination and assessment of albuminuria was performed 3 days and 1 day prior to 8C2 injection. Mice were dosed 8C2 (10 mg/kg) via intravenous penile vein injection. Blood samples (20 μl) were collected from the saphenous vein, submandibular vein, or retro-orbital plexus at 3, 9, 24, 48, 96, and 168 h. 8C2 concentrations were determined by validated ELISA.

### Data Analysis

One-way ANOVA, followed by pair-wise comparisons using Dunnett's post-hoc analyses, were performed to test the statistical significance of differences between treatment groups and controls. Statistical significance was set at a threshold of $P<0.05$. 8C2 pharmacokinetic data was analyzed by standard noncompartmental analysis in Phoenix WinNonlin 6.1 (Pharsight, Mountain View, CA).

### 8C2 Population Pharmacokinetic Modeling

To better understand the relationship between UAE and 8C2 plasma clearance, concentration time data was evaluated through pharmacokinetic population modeling with the Stochastic Approximation Expectation Maximization (SAEM) algorithm within MONOLIX 4.1.4 (25). The structural model (Fig. 1) was modeled as a two compartment mammillary model with linear distribution and elimination. The following parameters were estimated: systemic clearance (CL), central compartment volume ($V_1$), volume of the tissue compartment ($V_2$), and intercompartmental distribution clearance ($CL_d$).

$$V_1 \cdot \frac{dC_1}{dt} = CL_d \cdot C_2 - (CL_d + CL) \cdot C_1 \quad IC = Dose / Vi \quad (1)$$

$$V_2 \cdot \frac{dC_2}{dt} = CL_d \cdot (C_1 - C_2) \quad IC = 0 \quad (2)$$

Interindividual variability (IIV) in CL, $CL_d$, $V_1$, and $V_2$ was modeled with an exponential variance model:

$$P_j = P_{pop} \cdot e^{\eta_j} \quad (3)$$

where $P_j$ and $P_{pop}$ represent the parameter estimate of the jth animal and the typical parameter population estimate. $\eta_j$ is the IIV in the jth animal, with a normal distribution centered around 0, and a variance of $\omega^2$. Residual variability was modeled with a proportional error model:

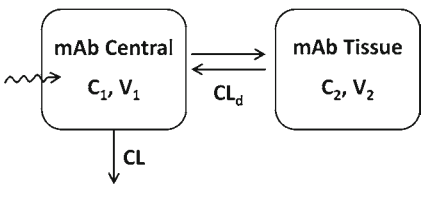


**Fig. 1** A schematic representation of the base pharmacokinetic model for 8C2 antibody disposition. Antibody is dosed intravenously into the central compartment. Linear antibody elimination clearance (CL) is assumed to occur solely from the central compartment. Linear distribution clearance ($CL_d$) occurs between the central and peripheral tissue compartment. $V_1$ and $V_2$ represent the volumes of distribution of the central and peripheral tissue compartment respectively.

$$C_{ij} = \hat{C}_{ij} \cdot (1 + \varepsilon_{ij}) \quad (4)$$

where $C_{ij}$ is the ith measured 8C2 plasma concentration in the jth animal, and $\hat{C}_{ij}$ is the ith model predicted 8C2 plasma concentration in the jth animal. $\varepsilon_{ij}$ is a normally distributed variable centered around 0 that equals the difference in the ith obvserved and model predicted 8C2 plasma concentration in the jth animal.

The covariate relationship of UAE on CL was modeled with a power model centered by the covariate mean:

$$CL_j = CL_{pop} \cdot \left(\frac{UAE_j}{UAE_m}\right)^{\theta_{CL}} \quad (5)$$

where $CL_j$ and $CL_{pop}$ are the clearance estimate of the jth animal and the typical clearance population estimate, and where $UAE_j$ is the urinary albumin excretion of the jth animal. $UAE_m$ represents the mean urinary albumin excretion in the sampled population. $\Theta_{CL}$ is the exponential unitless covariate parameter that is used to fit the relationship between UAE and CL.

## RESULTS

### GFR of STZ-Treated Mice

GFR was measured in mice after a single bolus injection of FITC-inulin 3 days prior to 8C2 administration. The terminal phase of decline of plasma FITC-inulin is representative of GFR in this system. Individual mouse GFR ranged from 0.365 to 0.696 ml/min, and was found to increase with time after STZ-treatment (Fig. 2). GFR increase was statistically significant (one-way ANOVA with Dunnett's post-hoc test: $p < 0.01$) between the control group (0.421 ± 0.031 ml/min) and 3, 4, and 6-week STZ-treatment groups (0.552 ± 0.084, 0.584 ± 0.079, and 0.584 ± 0.078 ml/min), with an increase of 39% between control and the 6-week STZ-treatment group. GFR of all groups are shown in Table I. The trend of GFR with time after STZ-treatment is in agreement with previous work, and is indicative loss of renal barrier function (26).

### UAE of STZ-Treated Mice

UAE was measured by indirect competitive ELISA, with a urine collection period of 24 h, performed 1 day prior to 8C2 administration. UAE ranged from 20.1 to 121 μg/day (Fig. 2). The UAE observed in mice within the 2, 3, 4, and 6-week STZ-treatment groups (Average ± SD) were: 35.9 ± 7.9, 49.8 ± 9.5, 82.9 ± 11.2, and 99.3 ± 13.7 μg/day (one-way ANOVA with Dunnett's post-hoc test: $p < 0.01$), relative to the control group (25.7 ± 3.3 μg/day). Comparing the 6-week STZ-treatment group to the control group, there was 286% increase in UAE (Table I). The increased UAE with STZ-treatment signifies a loss of kidney barrier function, consistent with previous literature reports (26).

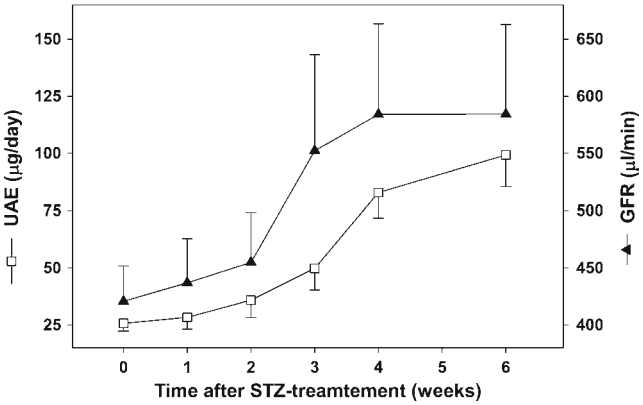


**Fig. 2** Urinary albumin excretion rate —□— (y-axis left), and glomerular filtration rate —▲— (y-axis right) increase with time after STZ-treatment. *Data points* and *error bars* represent mean and standard deviation.

### 8C2 Pharmacokinetic Studies in STZ-Induced Mice

After intravenous dosing of 10 mg/kg 8C2, plasma samples were collected at 3, 9, 24, 48, 96, and 168 h and analyzed via ELISA. Individual plasma samples displayed typical biexponential pharmacokinetic profiles (Fig. 3a). Individual concentration *vs*. time data were analyzed by traditional non-compartmental analysis and results were stratified by STZ-treatment group (Table I). The NCA-calculated steady state volume of distribution was relatively consistent across test groups, with a mean ± SD of 133 ± 6.9 ml/kg. The mean 8C2 clearance for the 6-week STZ-treatment group was increased 88% relative to the value found from the control group (Fig. 3b). Animals that received 8C2 3–6 weeks after STZ-treatment displayed significantly (one-way ANOVA with Dunnett's post-hoc test: $p < 0.01$) increased 8C2 clearance (0.229 ± 0.066–0.228 ± 0.061 ml/hr/kg) relative to control animals (0.121 ± 0.0125 ml/hr/kg). NCA-calculated 8C2 clearance was highly correlated with UAE and GFR (Pearson's Correlation Coefficients: 0.731 and 0.771 respectively).

### Population Pharmacokinetic Modeling of 8C2 Pharmacokinetic Data in STZ-Induced Mice

The 8C2 plasma concentration data, in combination with individual estimates for GFR and UAE, were used to build a population pharmacokinetic model to both better describe the data, and to evaluate covariate relationships between 8C2

**Table I** NCA Derived 8C2 Pharmacokinetic Parameters (CL and $V_{ss}$), UAE, and GFR - Stratified by Time After STZ-treatment

[a] Values are listed as mean ± standard deviation

| Parameters[a] | Week 0 | Week 1 | Week 2 | Week 3 | Week 4 | Week 6 |
|---|---|---|---|---|---|---|
| CL *(μl/hr/kg)* | 121 ± 13 | 100 ± 30 | 136 ± 76 | 220 ± 66 | 229 ± 58 | 228 ± 61 |
| $V_{SS}$ *(ml/kg)* | 138 ± 6.2 | 140 ± 3.8 | 135 ± 5.1 | 132 ± 4.4 | 127 ± 6.0 | 130 ± 6.9 |
| UAE *(μg/day)* | 25.7 ± 3.3 | 28.3 ± 5.1 | 35.9 ± 7.5 | 49.8 ± 9.5 | 82.9 ± 11 | 99.3 ± 14 |
| GFR *(ml/min/kg)* | 12.9 ± 0.95 | 13.4 ± 0.95 | 14.0 ± 1.3 | 16.9 ± 2.6 | 17.9 ± 2.4 | 17.9 ± 2.4 |

pharmacokinetics and markers of renal function. A two-compartment mammillary base model was used to characterize 8C2 plasma pharmacokinetic data. Estimates of fixed effects, IIV, and residual variability are shown in Table II. Notably, the IIV of total clearance was estimated to be 35.9%, at least three times greater than the model estimated IIV of every other parameter.

To test the contribution of renal function on the IIV of CL, an individual parameter of renal function was tested as a covariate on the base model. Proteinuria has been shown to increase monotonically with progression of nephropathy. Conversely, GFR first rises, and then decreases. In this model system, addition of GFR as a covariate on CL improves model fit similar to the addition of UAE as a covariate on CL (data not shown). Use of both covariates in the model had no increased benefit due to the high correlation between UAE and GFR. Given the complex relationship between GFR and the severity of nephropathy, and given the strong correlation between GFR and UAE (Fig. 2), UAE was singly applied as a covariate on CL. The addition of UAE to the base model decreased the objective function from 1787 (base model) to 1735 (final model). Goodness-of-fit plots show good model fit of both population-predicted 8C2 concentration (Fig. 4a) and individual predicted 8C2 concentration (Fig. 4b) with observed 8C2 plasma concentration. The addition of UAE as a covariate reduced the unexplained residual variability in CL (IIV) from 35.9% to 21.8%. This is graphically shown by plotting $\eta_{CL,j}$ *vs*. $UAE_j$ for the base model (Fig. 5a) and for the final model (Fig. 5b), with a loss of trend seen in the final model plot.

## DISCUSSION

Approximately ~40% of patients with diabetes develop diabetic nephropathy (27,28), which is characterized by glomerular sclerosis, and progressively worsening albuminuria (29,30). It is expected that there will be ~28 million people with diabetes in 2013 in the United States, with approximately ~304 million expected worldwide (31). Due to the predicted growth in the global population of diabetic patients (32), and due to the high fraction of diabetic patients that develop nephropathy, the impact of this condition on the safety and efficacy of drug therapy is a substantial concern.

Diabetic nephropathy has been categorized in five stages (33). Stage 1 is characterized by early hyperfunction and

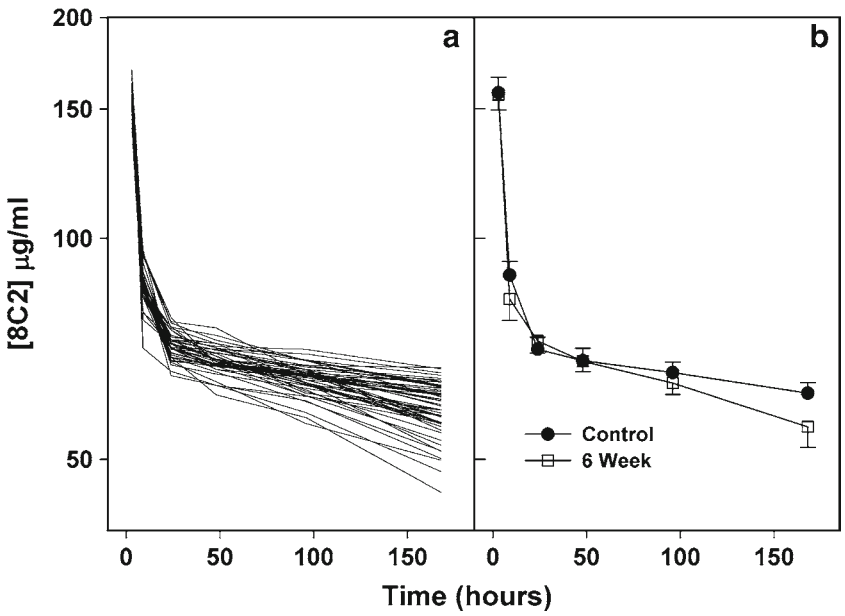


**Fig. 3** Plasma concentration (*μg*/ml) *vs*. time (hours) profiles following an intravenous dose of 10 mg/kg in male Swiss Webster mice. (**a**) Individual plasma concentration (*μg*/ml) *vs*. time (hours) profiles for all mice (control, 1, 2, 3, 4, or 6 weeks after STZ-treatment) following an intravenous dose of 10 mg/kg shows pharmacokinetic variability in population. (**b**) STZ-treatment (6 weeks) results in an increase in terminal elimination slope compared to control mice (no STZ-treatment). *Data points* and *error bars* represent mean and standard deviation.

**Table II** Population Pharmacokinetic Model Derived Parameters for 8C2 in STZ-treated Mice for the bBse and Final Models

| Parameter | Base model | | Final model | |
|---|---|---|---|---|
| | Estimate | %RSE | Estimate | %RSE |
| Fixed effects | | | | |
| CL *(μl/hr/kg)* | 168 | 5 | 180 | 3 |
| $V_1$ *(ml/kg)* | 34.3 | 2 | 34.3 | 2 |
| $V_2$ *(ml/kg)* | 98.6 | 1 | 98.7 | 2 |
| $CL_d$ *(μl/hr/kg)* | 7760 | 1 | 7750 | 1 |
| $\Theta_{UAE,CL}$ | – | – | 0.564 | 12 |
| IIV[a] | | | | |
| IIV on CL *(%)* | 35.9 | 11 | 21.8 | 13 |
| IIV on $V_1$ *(%)* | 9.79 | 14 | 11.1 | 12 |
| IIV on $V_2$ *(%)* | 5.71 | 12 | 6.30 | 11 |
| IIV on $CL_d$ *(%)* | 8.40 | 12 | 8.90 | 11 |
| Residual variability | | | | |
| Proportional error (%) | 2.28 | 6 | 2.08 | 6 |
| Objective function | 1787 | | 1735 | |

*CL* systemic clearance, $V_1$ central compartment volume, $V_2$ volume of the tissue compartment, $CL_d$ intercompartmental distribution clearance, $\Theta_{CL}$ exponential covariate parameter, *IIV* interindividual variability

[a] IIV expressed as: $CV\% = \sqrt{\exp(\omega^2)-1}$

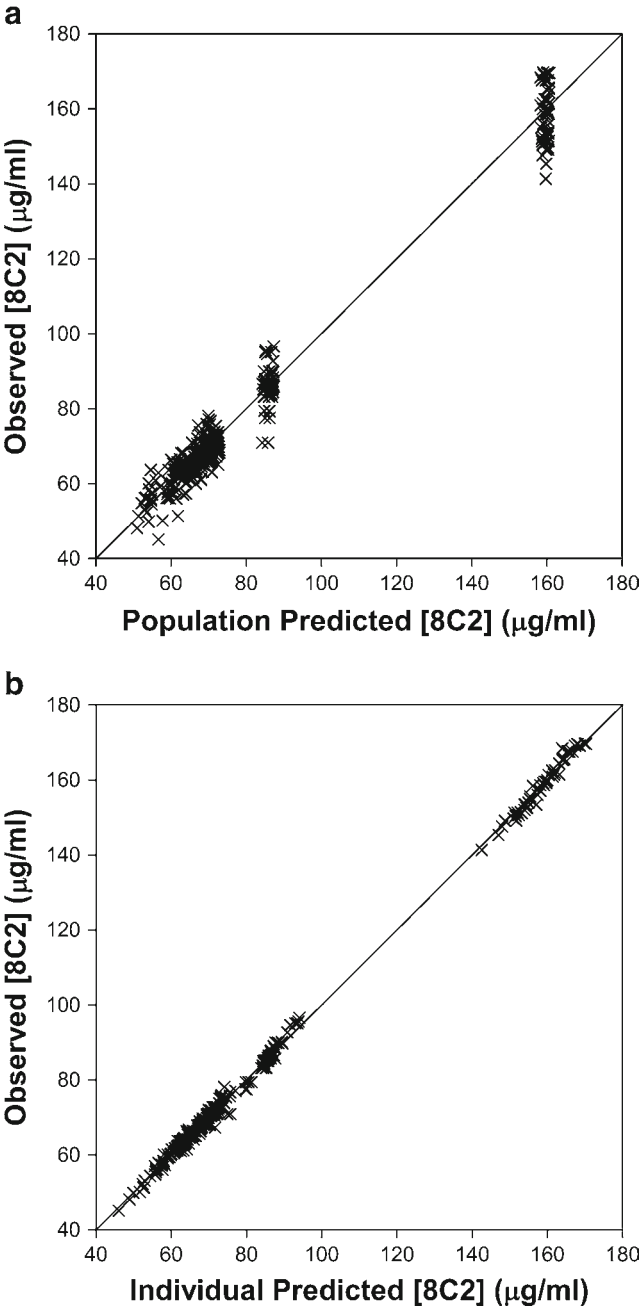


**Fig. 4** Goodness-of-fit plots for final 8C2 plasma pharmacokinetic model. (**a**) Observed 8C2 plasma concentration *vs*. population predicted 8C2 plasma concentration. (**b**) Observed 8C2 plasma concentration *vs*. individual predicted 8C2 plasma concentration. The *solid line* represents the line of identity in plots (**a**) and (**b**).

hypertrophy. Stage 2 is associated with morphologic lesions without signs of clinical disease, and by increased glomerular filtration rate (GFR). In Stage 3, incipient diabetic nephropathy, urinary albumin excretion is significantly elevated to 15–300 ug/min. Stage 4 is overt diabetic nephropathy, characterized by the presence of proteinuria >0.5 g/24 h and declining GFR (The mean fall rate being around 1 ml/min/mo). Stage 5 is end-stage renal failure with uremia due to diabetic nephropathy. The majority of patients with diabetic nephropathy are categorized clinically as early stage (34–36); however, 30–45% of patients with early stage (microalbuminuric) diabetic nephropathy will progress to late stage nephropathy within 10 years (37).

The STZ mouse model mimics the pathologic kidney damage seen in patients with mild diabetic nephropathy, correlating to Stage 2 or Stage 3. This includes accumulation of macrophages, microalbuminuria, glomerulosclerosis, and tubulointerstitial fibrosis (38). The present study utilized a maximum inducement time of 6 weeks, as it has been previously shown that peak values for UAE and GFR occur 6–8 weeks after STZ-treatment in this animal model (26). Increased inducement time does not result in further increases in UAE, or to decreases in GFR (as would be typical for late stage diabetic nephropathy). Therefore, this model is limited to the study of early stages of diabetic nephropathy (26).

Multiple physiological changes have been associated with the onset and progression of diabetic nephropathy, including increased plasma concentrations of inflammatory molecules and growth factors, increased oxidative stress, and alterations in metabolic pathways (40). Progression of diabetic nephropathy has been correlated to increased systemic blood pressure and to increased intra-glomerular pressure (40). At the present time, there is an incomplete understanding of the mechanisms responsible for the observed increase in urinary IgG excretion, and for the observed increase in 8C2 plasma clearance, in subjects with diabetic nephropathy. However, considering the

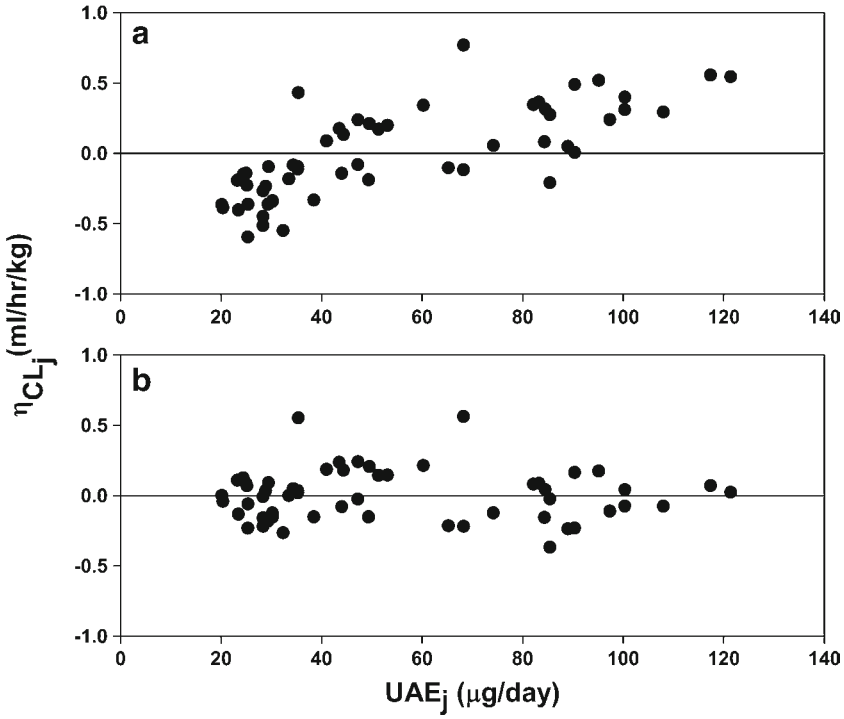


**Fig. 5** Random effects for clearance ($\eta_{CL_j}$) relative to urinary albumin excretion ($UAE_j$) compared for base model without (**a**) and final model with $UAE_j$ covariate effect on $CL_j$ (**b**). Inclusion of covariate in final model resulted in minimization of trend in eta plot (**b**), and reduction of unexplained residual variability of total clearance (CL).

known pathophysiological changes associated with diabetic nephropathy, it is likely that increased IgG excretion is primarily explained by decreased glomerular permaselectivity.

The permeability and selectivity of the glomerulus is determined by the structural characteristics of the glomerular capillary membrane. The overall negative charge of this membrane, combined with its size-restrictive effective pore size, contribute to the poor permeability of large anionic proteins like albumin and IgG (39). Nephropathy leads to pathological changes in the kidney, including accumulation of extracellular matrix and the infiltration of inflammatory cells into glomerli and into tubulointerstitial spaces (39). Multiple reports show that these pathological changes to the kidney result in loss of permaselectivity to plasma proteins, including IgG (18–20,41–43). These changes are marked by indicators of renal function, including increased UAE, and altered GFR.

Creatinine clearance (CLcr) is commonly employed in clinical practice as an indicator of renal function and as a measure of GFR. Assessment of CLcr typically involves the collection of a single blood sample, which is assayed to determine the concentration of creatinine in serum. The measured serum creatinine concentration, which is assumed to be reflective of "steady-state", is then related to an estimated rate of creatinine production (typically estimated based on patient weight and age) to estimate CLcr and, thus, GFR. Although this method is easy and convenient, there are several limitations. First, the rate of endogenous creatinine production shows significant inter-individual variation, which is not completely explained by variation in age and weight (e.g., relating to variation in muscle mass, race, and disease state (44)). Moreover, CLcr is not an ideal measure of GFR, as creatinine undergoes active tubular secretion and tubular reabsorption (44). Additionally, with respect to the goals of the current work, quantification of creatinine concentrations in mice is complicated by the presence of high levels of non-creatinine chromagens in mouse blood (45,46). Owing to these difficulties and limitations, we chose to use inulin clearance as a marker of GFR in this work. Clearly, the evaluation of inulin clearance is more demanding, from a technical standpoint, relative to the assessment of CLcr, as the evaluation requires the administration of inulin and the collection of several blood samples. Nonetheless, inulin clearance is widely considered as the "gold standard" measure of GFR, as inulin is biologically inert, unbound by plasma protein, freely filtered by the glomerulus, and neither reabsorbed, metabolized, nor secreted by the kidneys (39).

Albuminuria is a central manifestation of diabetic nephropathy. The occurrence of albuminuria is a reflection of increased matrix deposition, leading to glomerular and tubulointerstitial lesions. Clinically, diabetic nephropathy is didactically categorized into stages based on the values of UAE; i.e., microalbuminuria (20–300 mg/day) and macroalbuminuria (>300 mg/day) (47). Therefore, UAE is an important indicator of renal function and to define stage of diabetic nephropathy. In this study, UAE became elevated 2 weeks after STZ-treatment, indicating onset of early-stage nephropathy. The time-course of STZ-induced renal

impairment observed in our work is consistent with published data from studies of mice and rats (26).

8C2 CL correlated well with increasing GFR and UAE, indicating that mAb CL increases with renal injury in the STZ mouse model of diabetic nephropathy. Due to the initial increase, followed by a progressive decrease, in GFR in early human kidney disease progression, GFR may not be a suitable biomarker of renal function for prediction of therapeutic protein renal CL. Conversely, UAE has better potential as a clinical biomarker, as it increases monotonically with progression of diabetic nephropathy. In this study, UAE increase was significant 2 weeks post STZ-treatment, and reached a maximum 3.8-fold increase relative to control 6 weeks after STZ-treatment. This corresponded to an 88% increase in total clearance of 8C2 in mice 6 weeks after STZ-treatment relative to controls. The degree of renal impairment in this animal model is conservative relative to human diabetic nephropathy, where UAE is typically increased 100–1,000 fold in humans with micro or macro-albuminuria. Consequently, it is reasonable to expect a more dramatic increase in the clearance of therapeutic mAbs in patients with nephropathy (*vs*. the increase in 8C2 clearance observed in this work).

The use of markers of renal function as covariates has been extensively explored in small molecule population pharmacokinetic models to explain residual variability and to improve the precision of model predictions for individual patients. With use of a therapeutic mAb in an animal model of diabetic nephropathy, a simple population pharmacokinetic model with UAE as a covariate on 8C2 CL resulted in better model fit, and explained much of the residual variability associated with 8C2 CL. Similar approaches with therapeutic mAbs may find utility in subsets of patients with renal impairment to account for variability in large clinical datasets, and to facilitate efforts to individualize dosing.

There is some clinical evidence suggesting that early stage nephropathy may have a significant impact on therapeutic mAb CL. Rituximab, a chimeric monoclonal antibody that selectively depletes B-cells, has been used off-label to treat idiopathic membranous nephropathy (IDM). IDM patients with increased UAE were found to exhibit rituximab serum concentrations that were significantly lower than concentrations observed in non-proteinuric patients with rheumatoid arthritis (who were given the same dosing regimen, and with assay performed with the same method, $p < 0.001$) (48). It is quite possible, and perhaps quite likely, that nephropathy contributes significantly to interindividual variability in clearance for several monoclonal antibody drugs.

In conclusion, this study demonstrated that early stage, STZ-induced diabetic nephropathy was associated with a significant increase in the clearance of 8C2, a model monoclonal antibody. The clearance of 8C2 was positively correlated with UAE and GFR, markers of early stage nephropathy. The use of a population based pharmacokinetic model accounted for residual variability of CL, suggesting the potential for employment of similar models to explain and predict the contribution of diabetic nephropathy to the interindividual variability in mAb CL in patients. Similar studies with preclinical models of later stage nephropathy, as well as clinical studies, appear to be justified.

## ACKNOWLEDGMENTS AND DISCLOSURES

This study was supported by a grant from the Center for Protein Therapeutics.

## REFERENCES

1. Leader B, Baca QJ, Golan DE. Protein therapeutics: a summary and pharmacological classification. Nat Rev Drug Discov. 2008;7:21–39.
2. Reichert JM. Metrics for antibody therapeutics development. MAbs. 2010;2:695–700.
3. Rojas R, Apodaca G. Immunoglobulin transport across polarized epithelial cells. Nat Rev Mol Cell Biol. 2002;3:944–55.
4. McCarthy KM, Lam M, Subramanian L, Shakya R, Wu Z, Newton EE. Effects of mutations in potential phosphorylation sites on transcytosis of FcRn. J Cell Sci. 2001;114:1591–8.
5. Antohe F, Radulescu L, Gafencu A, Ghetie V, Simionescu M. Expression of functionally active FcRn and the differentiated bidirectional transport of IgG in human placental endothelial cells. Hum Immunol. 2001;62:93–105.
6. Praetor A, Ellinger I, Hunziker W. Intracellular traffic of the MHC class I-like IgG Fc receptor, FcRn, expressed in epithelial MDCK cells. J Cell Sci. 1999;112(Pt 14):2291–9.
7. Ward ES, Zhou J, Ghetie V, Ober RJ. Evidence to support the cellular mechanism involved in serum IgG homeostasis in humans. Int Immunol. 2003;15:187–95.
8. Junghans RP, Anderson CL. The protection receptor for IgG catabolism is the beta2-microglobulin-containing neonatal intestinal transport receptor. Proc Natl Acad Sci U S A. 1996;93:5512–6.
9. Raghavan M, Chen MY, Gastinel LN, Bjorkman PJ. Investigation of the interaction between the class I MHC-related Fc receptor and its immunoglobulin G ligand. Immunity. 1994;1:303–15.
10. Brambell FW, Hemmings WA, Morris IG. A theoretical model of gamma-globulin catabolism. Nature. 1964;203:1352–4.
11. Tabrizi MA, Tseng CM, Roskos LK. Elimination mechanisms of therapeutic monoclonal antibodies. Drug Discov Today. 2006;11:81–8.
12. Levy G. Pharmacologic target-mediated drug disposition. Clin Pharmacol Ther. 1994;56:248–52.
13. Vugmeyster Y, Xu X, Theil FP, Khawli LA, Leach MW. Pharmacokinetics and toxicology of therapeutic proteins: advances and challenges. World J Biol Chem. 2012;3:73–92.
14. Dirks NL, Meibohm B. Population pharmacokinetics of therapeutic monoclonal antibodies. Clin Pharmacokinet. 2010;49:633–59.
15. Davies B, Morris T. Physiological parameters in laboratory animals and humans. Pharm Res. 1993;10:1093–5.
16. Crommelin DJA, Sindelar RD. Pharmaceutical biotechnology: an introduction for pharmacists and pharmaceutical scientists. London; New York: Routledge; 2002.
17. Woo KT, Lau YK. Proteinuria: clinical significance and basis for therapy. Singap Med J. 2001;42:385–9.

18. Bakoush O, Tencer J, Tapia J, Rippe B, Torffvit O. Higher urinary IgM excretion in type 2 diabetic nephropathy compared to type 1 diabetic nephropathy. Kidney Int. 2002;61:203–8.
19. Lemley KV, Blouch K, Abdullah I, Boothroyd DB, Bennett PH, Myers BD, *et al*. Glomerular permselectivity at the onset of nephropathy in type 2 diabetes mellitus. J Am Soc Nephrol. 2000;11:2095–105.
20. Mistry K, Kalia K. Non enzymatic glycosylation of IgG and their urinary excretion in patients with diabetic nephropathy. Indian J Clin Biochem. 2009;24:159–65.
21. Zhu Y, Hu C, Lu M, Liao S, Marini JC, Yohrling J, *et al*. Population pharmacokinetic modeling of ustekinumab, a human monoclonal antibody targeting IL-12/23p40, in patients with moderate to severe plaque psoriasis. J Clin Pharmacol. 2009;49:162–75.
22. Chen J, Lu Q, Balthasar JP. Mathematical modeling of topotecan pharmacokinetics and toxicodynamics in mice. J Pharmacokinet Pharmacodyn. 2007;34:829–47.
23. Shah D. Pharmacokinetic strategies to improve the safety and efficacy of intraperitoneal chemotherapy, Pharmaceutical Sciences, Vol. Doctor of Philosophy, University at Buffalo 2010, p. 585.
24. Qi Z, Whitt I, Mehta A, Jin J, Zhao M, Harris RC, *et al*. Serial determination of glomerular filtration rate in conscious mice using FITC-inulin clearance. Am J Physiol Renal Physiol. 2004;286:F590–6.
25. Lixsoft. Modelling & Simulation for Drug Development. http://www.monolix.org/ (accessed 2013 March 12 2013).
26. Qi Z, Fujita H, Jin J, Davis LS, Wang Y, Fogo AB, *et al*. Characterization of susceptibility of inbred mouse strains to diabetic nephropathy. Diabetes. 2005;54:2628–37.
27. Gross JL, de Azevedo MJ, Silveiro SP, Canani LH, Caramori ML, Zelmanovitz T. Diabetic nephropathy: diagnosis, prevention, and treatment. Diabetes Care. 2005;28:164–76.
28. Ritz E, Orth SR. Nephropathy in patients with type 2 diabetes mellitus. New Engl J Med. 1999;341:1127–33.
29. Young BA, Maynard C, Boyko EJ. Racial differences in diabetic nephropathy, cardiovascular disease, and mortality in a national population of veterans. Diabetes Care. 2003;26:2392–9.
30. Tarnow L, Rossing P, Nielsen FS, Fagerudd JA, Poirier O, Parving HH. Cardiovascular morbidity and early mortality cluster in parents of type 1 diabetic patients with diabetic nephropathy. Diabetes Care. 2000;23:30–3.
31. Shaw JE, Sicree RA, Zimmet PZ. Global estimates of the prevalence of diabetes for 2010 and 2030. Diabetes Res Clin Pract. 2010;87:4–14.
32. Herman WH, Zimmet P. Type 2 diabetes: an epidemic requiring global attention and urgent action. Diabetes Care. 2012;35:943–4.
33. Mogensen CE, Christensen CK, Vittinghus E. The stages in diabetic renal disease. With emphasis on the stage of incipient diabetic nephropathy. Diabetes. 1983;32 Suppl 2:64–78.
34. Levey AS, de Jong PE, Coresh J, El Nahas M, Astor BC, Matsushita K, *et al*. The definition, classification, and prognosis of chronic kidney disease: a KDIGO Controversies Conference report. Kidney Int. 2011;80:17–28.
35. Bakris GL. Recognition, pathogenesis, and treatment of different stages of nephropathy in patients with type 2 diabetes mellitus. Mayo Clin Proc. 2011;86:444–56.
36. Gurley SB, Clare SE, Snow KP, Hu A, Meyer TW, Coffman TM. Impact of genetic background on nephropathy in diabetic mice. Am J Physiol Renal Physiol. 2006;290:F214–22.
37. Caramori ML, Fioretto P, Mauer M. The need for early predictors of diabetic nephropathy risk: is albumin excretion rate sufficient? Diabetes. 2000;49:1399–408.
38. Chow FY, Nikolic-Paterson DJ, Atkins RC, Tesch GH. Macrophages in streptozotocin-induced diabetic nephropathy: potential role in renal fibrosis. Nephrol Dial Transplant. 2004;19:2987–96.
39. Guyton AC, Hall JE. Textbook of medical physiology. Philadelphia: Elsevier Saunders; 2006.
40. Dronavalli S, Duka I, Bakris GL. The pathogenesis of diabetic nephropathy. Nat Clin Pract Endocrinol Metab. 2008;4:444–52.
41. McQuarrie EP, Shakerdi L, Jardine AG, Fox JG, Mackinnon B. Fractional excretions of albumin and IgG are the best predictors of progression in primary glomerulonephritis. Nephrol Dial Transplant. 2011;26:1563–9.
42. Narita T, Fujita H, Koshimura J, Meguro H, Kitazato H, Shimotomai T, *et al*. Glycemic control reverses increases in urinary excretions of immunoglobulin G and ceruloplasmin in type 2 diabetic patients with normoalbuminuria. Horm Metab Res. 2001;33:370–8.
43. Deckert T, Feldt-Rasmussen B, Djurup R, Deckert M. Glomerular size and charge selectivity in insulin-dependent diabetes mellitus. Kidney Int. 1988;33:100–6.
44. Perrone RD, Madias NE, Levey AS. Serum creatinine as an index of renal function: new insights into old concepts. Clin Chem. 1992;38:1933–53.
45. Meneton P, Ichikawa I, Inagami T, Schnermann J. Renal physiology of the mouse. Am J Physiol Renal Physiol. 2000;278:F339–51.
46. Meyer MH, Meyer Jr RA, Gray RW, Irwin RL. Picric acid methods greatly overestimate serum creatinine in mice: more accurate results with high-performance liquid chromatography. Anal Biochem. 1985;144:285–90.
47. Molitch ME, DeFronzo RA, Franz MJ, Keane WF, Mogensen CE, Parving HH, *et al*. Nephropathy in diabetes. Diabetes Care. 2004;27:S79–83.
48. Fervenza FC, Cosio FG, Erickson SB, Specks U, Herzenberg AM, Dillon JJ, *et al*. Rituximab treatment of idiopathic membranous nephropathy. Kidney Int. 2008;73:117–25.